JOURNAL OF MATERIALS SCIENCE **30** (1995) 5915–5922

The wetting of silicon nitride by chromium-containing alloys

P. XIAO, B. DERBY
Department of Materials, University of Oxford, Parks Road, Oxford, OX1 3PH, UK

The wetting of ceramic materials by metallic melts is the most important characteristic of brazing alloys. The effect of chromium additions to copper-base alloys on the wetting of silicon nitride was investigated. Wetting experiments were carried out on Si_3N_4 using liquid Cu–Cr, Cu–Ni–Cr, Cu–Si–Cr and Cu–Ni–Si–Cr alloys. The addition of chromium to liquid copper up to its solubility limit promoted wetting on Si_3N_4. Improved wetting with a higher chromium content was achieved by the addition of nickel to the Cu–Cr alloys. The formation of an interfacial reaction layer, which is detrimental for brazing ceramics, was suppressed by the addition of silicon to the chromium-containing brazing alloys.

1. Introduction

In order to produce a good joint, brazing alloys must freely wet the surfaces to be joined. This condition is one of the most difficult to satisfy when designing a brazing alloy suitable for use with ceramics. In general, most metallic melts do not easily wet ceramic substrates and thus there is great interest in identifying alloy additions which promote wetting so as to develop suitable brazes for use with engineering ceramics. The addition of small quantities of titanium to a number of metal alloys can result in a dramatic increase in wettability [1–3] and a number of commercial brazing alloys have been developed on this principle. The presence of titanium in the liquid metal segregates to the liquid/solid interface and may promote a chemical reaction during the wetting process; with Si_3N_4, TiN and $TiSi_2$ form, TiC and $TiSi_2$ with SiC, and the suboxide TiO forms together with titanium intermetallics during the wetting of oxides by titanium-containing alloys [4]. TiC, TiN and TiO all show substantially metallic character bonding and previously it has been thought that it was the presence of this new metallic surface which promoted wetting [5], i.e. the presence of titanium in the melt converted the surface to a metal and the phenomenon was now one of a liquid metal wetting a solid metal surface. However, we have recently demonstrated that TiC and TiN are only readily wet by liquid metals when they have an extremely hypostoichiometric composition and it is not merely their metallic character which promotes wetting [6]. Thus the choice of "active" elements which promote the wetting of ceramics is probably not limited to those which show metallic character intermediate compounds with carbon, oxygen and nitrogen.

In this work we explore the effect of chromium additions to copper alloys as a means of promoting the wetting of Si_3N_4. Chromium is a highly reactive metal and forms carbide, nitride and oxide phases of high stability. The addition of chromium to nickel improves its wetting on Al_2O_3 without forming reaction products [7]. In this case wetting is believed to be caused by the segregation of CrO clusters to the solid/liquid interface. Here we investigate the effect chromium additions have on the wetting behaviour of copper alloys and the interface chemical composition.

2. Experimental procedure

We have used the sessile drop configuration to characterize wetting behaviour. In this case the contact (wetting) angle, θ, which encloses the liquid drop, is measured and related to the characteristic interfacial energies: γ_{SL} (solid/liquid), γ_{LV} (liquid/vapour) and γ_{SV} (solid/vapour), by the Young equation

$$\cos\theta = \frac{\gamma_{SV} - \gamma_{SL}}{\gamma_{LV}} \qquad (1)$$

The contact angle measurements were carried out using a dedicated vacuum furnace with an absolute pressure of about 5×10^{-6} mbar. A titanium sponge getter adjacent to the surface being characterized held the local oxygen partial pressure to about 10^{-25} bar.

Si_3N_4 polycrystalline plates (TenMat UK) were cut to size and polished flat using diamond slurries down to a final polishing grit size of 1 μm. The substrates were then cleaned in an ultrasonic bath with water and then with acetone before placing in the furnace. We used two different procedures to produce the metal samples used. Simple binary alloys of Cu–Si and Cu–Ni were fabricated in a vacuum melting furnace from pure metal mixtures (Goodfellow Metals, UK). These alloy pellets were, in turn, cut to size and cleaned before placing on the ceramic substrate. Binary Cu–Cr and more complex ternary and quaternary alloys were fabricated *in situ* during the sessile drop experiments by placing the individual elemental

0022–2461 © *1995 Chapman & Hall*

components in the appropriate ratio together on the substrate prior to heating. The precise composition of the alloy was then determined after each experiment by electron probe microanalysis of the solidified sessile drop.

For each experimental run the furnace was first heated to 100 °C and held to promote any outgassing of the specimen. The temperature was then increased at 10 °C min^{-1} to the desired temperature and then held for 45 min whilst measurements were made. The drop and substrate were then cooled to room temperature and sectioned for examination by optical microscopy. The cross-sections were also characterized by scanning electron microscopy (SEM) equipped with energy dispersive spectroscopy (EDS) and wavelength dispersive spectroscopy (WDS) for light element analysis.

3. Results

Fig. 1 shows the variation in contact angle with time measured from a Cu–3 wt % Cr alloy on Si_3N_4 at 1150 °C with the alloy forming *in situ* during the experiment. Note that all subsequent alloy compositions are in wt %. The relative position of the chromium and the copper on the substrate prior to the experiment affected the final results. If the chromium was placed on top of the copper pellet (Cr/Cu) there was little change in contact angle with time. However, if the small quantity of chromium was placed beneath the copper pellet (Cu/Cr), two types of behaviour were seen depending on the shape of the chromium. When the chromium was in the form of a thin foil (Cu/Cr1) we observed gas evolution or bubbling of the melt during wetting and measured a low equilibrium contact angle ($\theta \approx 40°$). If the chromium was present in the form of a more equiaxed lump (Cu/Cr2) we observed behaviour identical to the Cr/Cu configuration with an equilibrium contact angle close to 90°. Fig. 2 shows the change in equilibrium contact angle with increasing chromium content. There is a reduction in contact angle from 130° to 90° as 1% Cr is added to the alloy but further increases in chromium have no effect. This is consistent with the published Cr–Cu binary phase diagram (Fig. 3) which indicates a maximum solubility of slightly over 1.5% Cr in liquid copper at 1150 °C [8]. Thus, in all the high chromium content alloys the melt is saturated with chromium.

Metallographic cross-sections of the interface between the sessile drop and the Si_3N_4 substrate are shown in Fig. 4 for Cu–1%Cr and Cu–3% Cr. In both cases there is a clearly visible reaction layer which is slightly thicker in the Cu–3%Cr. In all cases of chromium content greater than 3%, a layer of undissolved chromium was visible at the top of the solidified droplet. Fig. 5 shows a WDS microanalytical line-scan across the metal/ceramic interface of the Cu–1% Cr sample. The reaction layer is chiefly Cr_2N although a copper silicide phase of unknown composition in partially included about 6 μm from the interface.

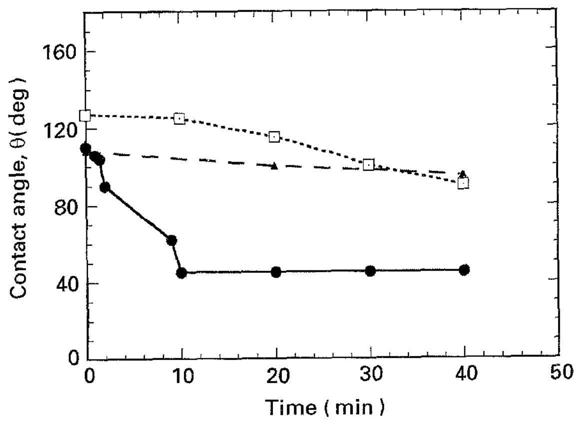

Figure 1 The variation of contact angle with time during wetting of Cu–3% Cr on Si_3N_4. Cu/Cr has copper above chromium on the substrate and Cr/Cu has chromium above copper. (●) Cu/Cr1, (□) Cr/Cu, (▲) Cu/Cr2.

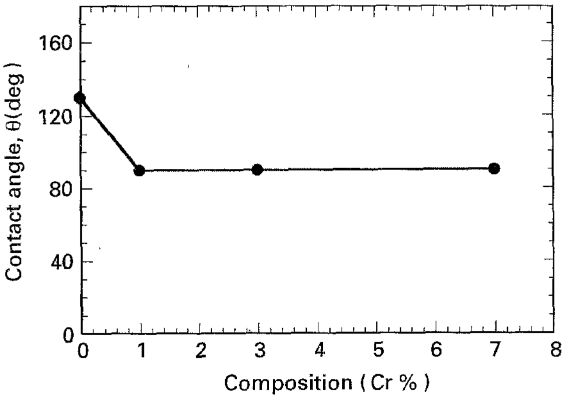

Figure 2 The variation of equilibrium contact angle with chromium content of Cu–Cr alloys on Si_3N_4, chromium above copper on the substrate.

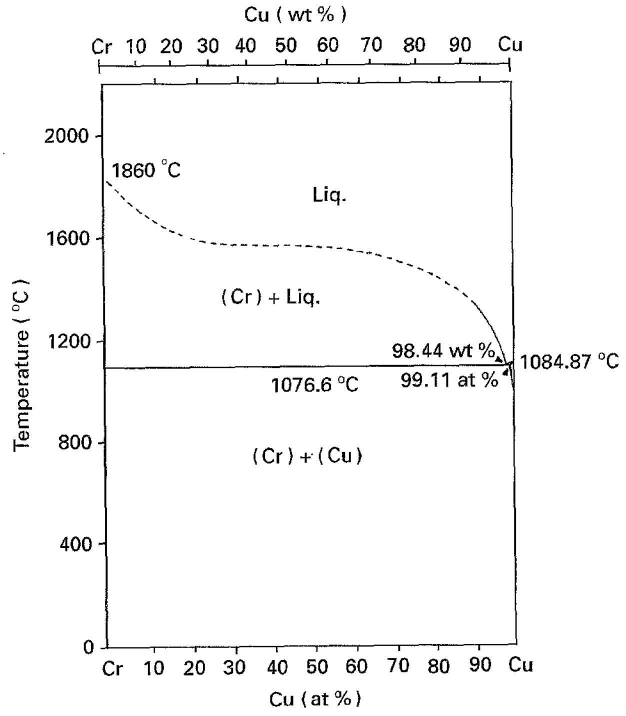

Figure 3 Schematic phase diagram of the Cu–Cr system redrawn from data in [8].

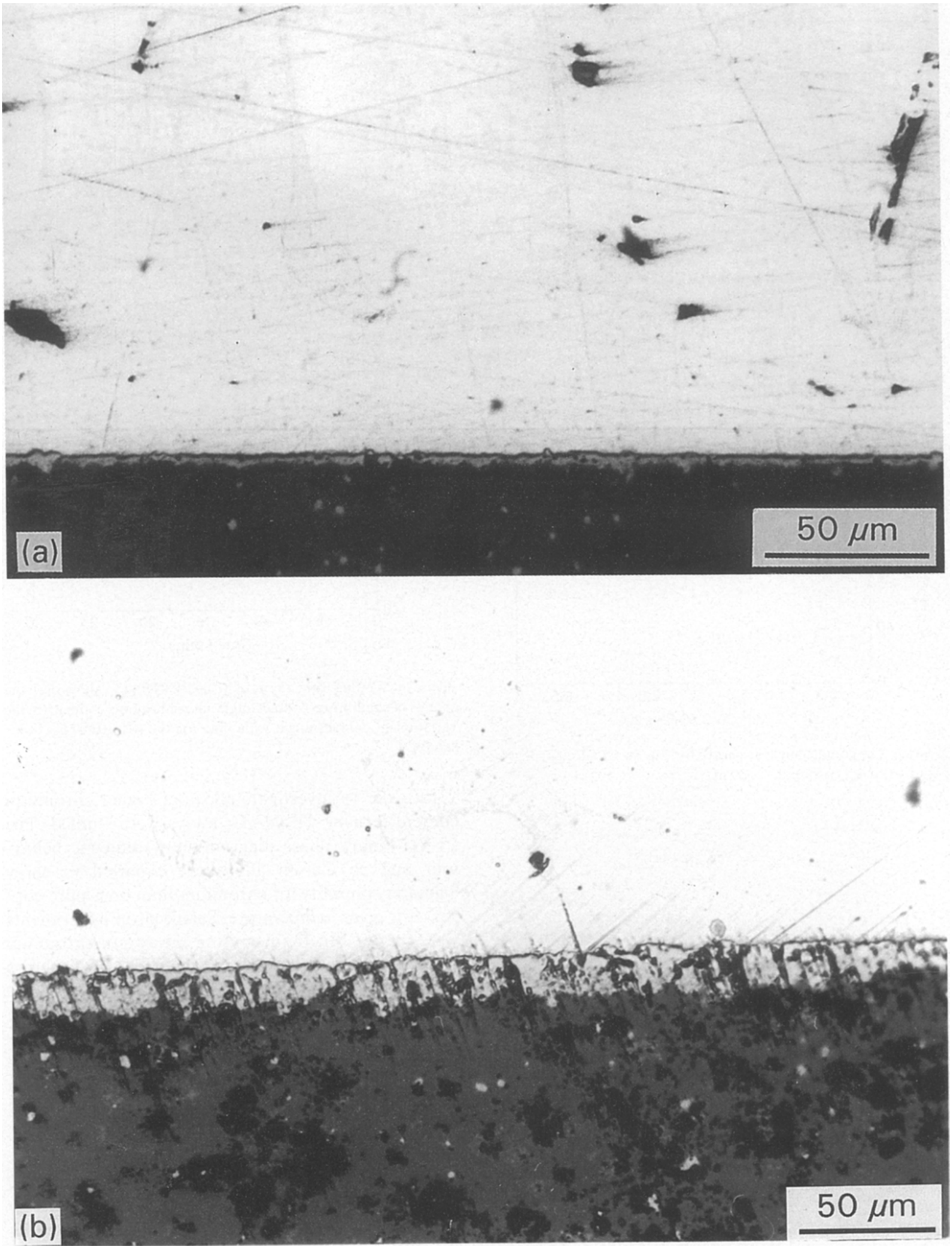

Figure 4 Cross-sections of the interface between the Si_3N_4 substrate and the solidified sessile drop. (a) Cu–1%Cr, (b) Cu–3%Cr.

The formation of Cr_2N at the interface is governed by the exchange reaction

$$8Cr_{(Cu)} + Si_3N_4 \rightleftharpoons 4Cr_2N + 3Si_{(Cu)} \qquad (2)$$

where the subscript (Cu) indicates an element in solution in the liquid copper alloy. Thus it should be possible to suppress the formation of Cr_2N at the interface if there is a sufficiently high silicon activity in the melt. This could be achieved by using a Cu–Cr–Si alloy. Fig. 6 shows the contact angle measured with Cu–Si–Cr alloys with increasing chromium content. All these alloys were produced by adding chromium to a Cr–5% Si master alloy. The behaviour is similar to that of the simple Cu–Cr binary alloy but now the

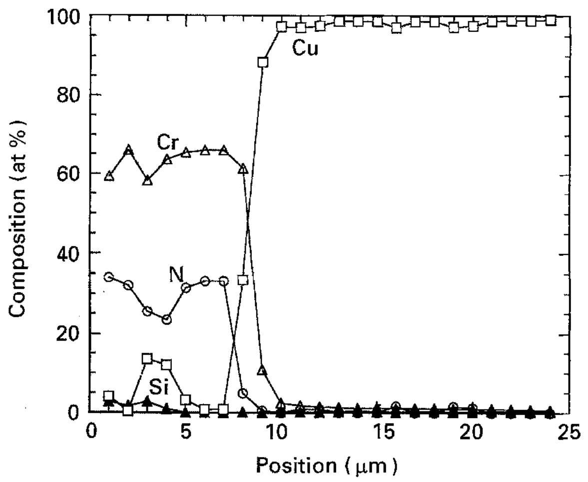

Figure 5 Microanalytical line-scan across the metal/ceramic interface of the Cu–1%Cr sample. (○) N, (▲) Si, (△) Cr, (□) Cu.

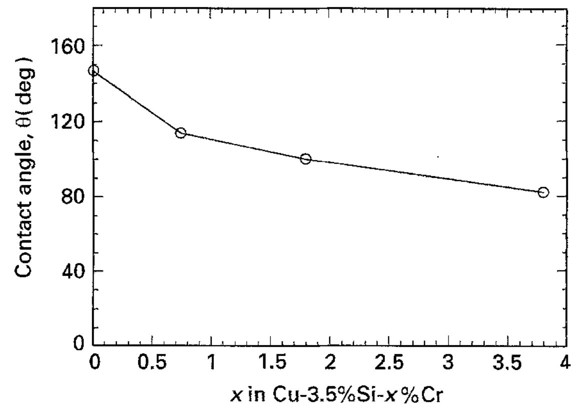

Figure 6 The contact angle measured for Cu–Si–Cr alloys on Si_3N_4 with increasing chromium content.

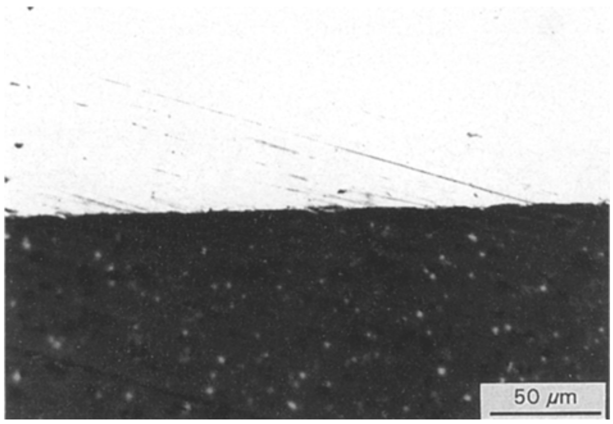

Figure 7 A cross-section from the Cu–5%Si–3.8%Cr/Si_3N_4 specimen.

minimum contact angle of 80° is achieved with 3.8%Cr. In the ternary Cu–Si–Cr system the maximum chromium solubility is about 3% and so no further improvement in wetting is expected. Fig. 7 shows a cross-section from the 3.8% Cr specimen. It is clear that Cr_2N formation has been suppressed. The light precipitates in the copper metal are either chromium silicides or silicon; both could be identified by microanalysis.

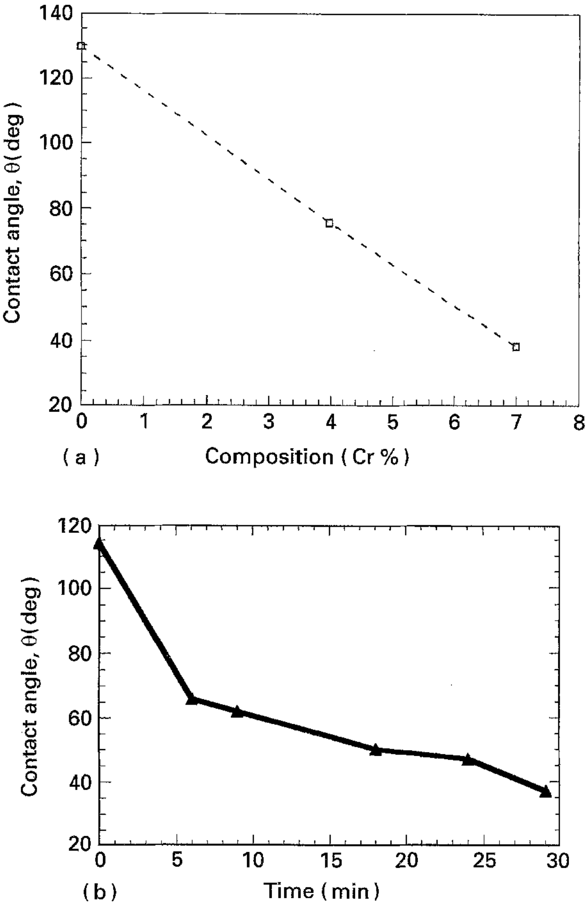

Figure 8 Wetting behaviour of (Cu–10%Ni)–Cr alloys; (a) the change of equilibrium contact angle with chromium, content; (b) the variation of contact angle with time for the (Cu–10%Ni)–7%Cr sample.

In order to investigate alloys of higher chromium content ternary Cu–Ni–Cr alloys were studied. The Cr–Ni binary phase diagram shows eutectic behaviour and so Cu–Ni alloys are expected to show a greater solubility for chromium than does pure copper at a given temperature. Sessile drop experiments were carried out by increasing the *in situ* chromium addition to a Cu–10% Ni master alloy. Fig. 8 shows the behaviour of two such (Cu–10%Ni)–Cr alloys. With 7% Cr, the contact angle decreases rapidly with time and reaches equilibrium at 40°, but with 4% Cr the angle is only reduced to 80° which is similar to the levels achieved with Cu–Cr and Cu–Si–Cr alloys which showed only limited solubility for chromium. Fig. 9 shows the interface cross-section from a (Cu–10% Ni)–7%Cr alloy. A thick reaction zone is visible which is confirmed as Cr_2N by WDS analysis.

Finally we consider a Cu–Ni–Si–Cr quaternary alloy. In this the chromium solubility is promoted by the presence of nickel and a sufficient silicon content is used to suppress Cr_2N formation. In these experiments we added small quantities of chromium to a Cu–20%Ni–5%Si master alloy. Fig. 10 shows the wetting angle as a function of chromium content and it it clearly seen that the effect of chromium addition is now dramatic with a contact angle measured below 20° for chromium contents greater than 3%. Fig. 11 shows interface cross-sections for (Cu–20% Ni–5%Si)–1.3%Cr and (Cu–20% Ni–5%Si)–5%Cr

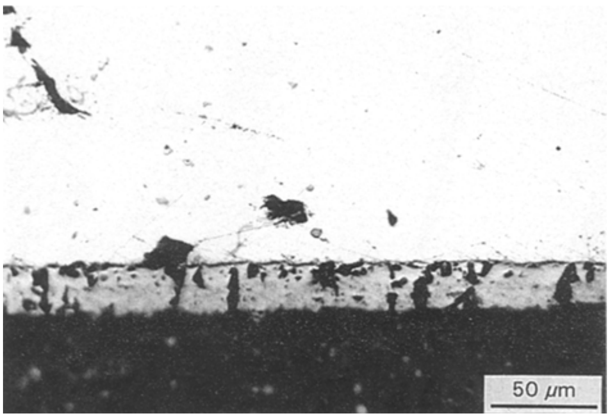

Figure 9 Cross-section from the (Cu–10 % Ni)–7 % Cr/Si_3N_4 specimen.

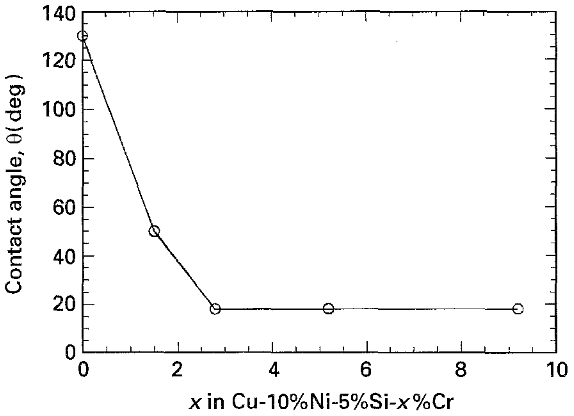

Figure 10 The change of equilibrium contact angle with chromium content measured for the (Cu–20 % Ni–5 % Si–Cr alloys.

droplets on Si_3N_4. In both cases there is no interfacial compound but there has been some attack of the Si_3N_4 surfaces which now appear rougher than in the earlier cross-sections. The large particles visible in the solidified metal of 5% Cr were identified as Cr_3Si, the smaller particles found near the interface in both specimens had a complex composition and contained significant quantities of nitrogen.

4. Discussion

Our results show only Cr_2N as a reaction product. No chromium silicide phases are formed at the interface and their presence in samples appears to come from rejection by the solidifying drop. The most stable silicide is $CrSi_2$ which has a Gibbs energy of $\Delta G = -72.2\ \text{kJ mol}^{-1}$ at 1200 °C [9]. If we consider a saturated Cu–Cr liquid we can take a chromium activity of 1. Our EDX results suggest a composition of about 0.3 at % Si for the binary droplet after solidification. If we take the Cu–Si binary interaction parameter for the liquid alloy of $-22.9\ \text{kJ mol}^{-1}$ [10], the activity of 0.3 at % Si is 5.0×10^{-4}. Thus a solution of 0.3% Si in a saturated Cu–Cr liquid should be stable without precipitating silicides at 1200 °C. However nitrogen has a very low solubility in liquid copper and the precipitation of Cr_2N occurs at the interface. Similar behaviour is expected for the Cu–Ni–Cr alloys. These results are different from the behaviour of Cu–Ti alloys on Si_3N_4, where both titanium silicides and nitrides are found at the metal/ceramic interface [1], and also for solid-state reactions between Ni–Cr alloys and Si_3N_4 where both chromium silicides and nitrides are found [11, 12].

Fig. 12 gives isothermal sections of the Cu–Si–Cr and Cu–Ni–Cr ternary phase diagrams, calculated using MTDATA [13]. The addition of quite small quantities of silicon lead to the formation of chromium silicides in equilibrium with the melt. The addition of 5 at % Si is also sufficient to prevent the formation of Cr_2N and keep the liquid in equilibrium with Si_3N_4. The maximum solubility of chromium in the binary Cu–Cr alloy is about 2 at %. The addition of nickel up to about 10 at % increases the solubility of chromium and this was accompanied by a decrease in the wetting angle of the Cu–Ni–Cr alloys on Si_3N_4. The addition of nickel decreases the activity of chromium in solution and a higher chromium concentration is needed for saturation. If we assume that wetting is controlled by adsorption of chromium to the interface, the increased concentration of chromium in the alloy may lead to a greater interfacial segregation.

There are insufficient data to calculate the complete Cu–Ni–Si–N–Cr phase diagram and thus we do not know the chromium activity in the quaternary alloys investigated. However, it is interesting to note the rather different reaction products with Cr_3Si and a complex phase precipitating in the droplet, presumably after solidification. The presence of nitrogen in the smaller particles near the interface and the roughening of the surface indicates a dissolution of Si_3N_4, but unlike the Cu–Cr and Cu–Ni–Cr alloys there is now significant nitrogen solubility in the liquid. The exceptional wetting in this system may be caused by the presence of Cr–N clusters at the interface analogous to the Cr–O clusters postulated for wetting of Ni–Cr alloys on oxides [7]. This presence of dissolved nitrogen may explain the improved wetting behaviour seen with these more complex alloys.

At present there is no accepted model describing the process of wetting concurrent with an interfacial reaction. However, reactive wetting can be simplified to the case of non-reactive wetting once the equilibrium contact angle is achieved. In this case, wetting occurs on the reaction product. One model has been proposed for the non-reactive wetting of oxides by liquid metals [16]. The work of adhesion, W_{adh}, of the metal Me on the oxide M_nO is related to the partial enthalpies of mixing at infinite dilution of oxygen and of M in the liquid Me, $\Delta H^{\infty}_{\text{O(Me)}}$, $\Delta H^{\infty}_{\text{M(Me)}}$

$$W = -\frac{c}{N^{1/3}V_{\text{Me}}^{2/3}}\left[\Delta H^{\infty}_{\text{O(Me)}} + \frac{1}{n}\Delta H^{\infty}_{\text{M(Me)}}\right] \qquad (3)$$

where N is Avogadro's number, V_{Me} is the atomic volume of the metal and c is an empirical constant ($c = 0.2$ for oxides). This equation gives reasonable agreement with experimental results for the wetting of oxides by pure liquid metals. Owing to the limited experiment data of wetting on nitrides or carbides, it is

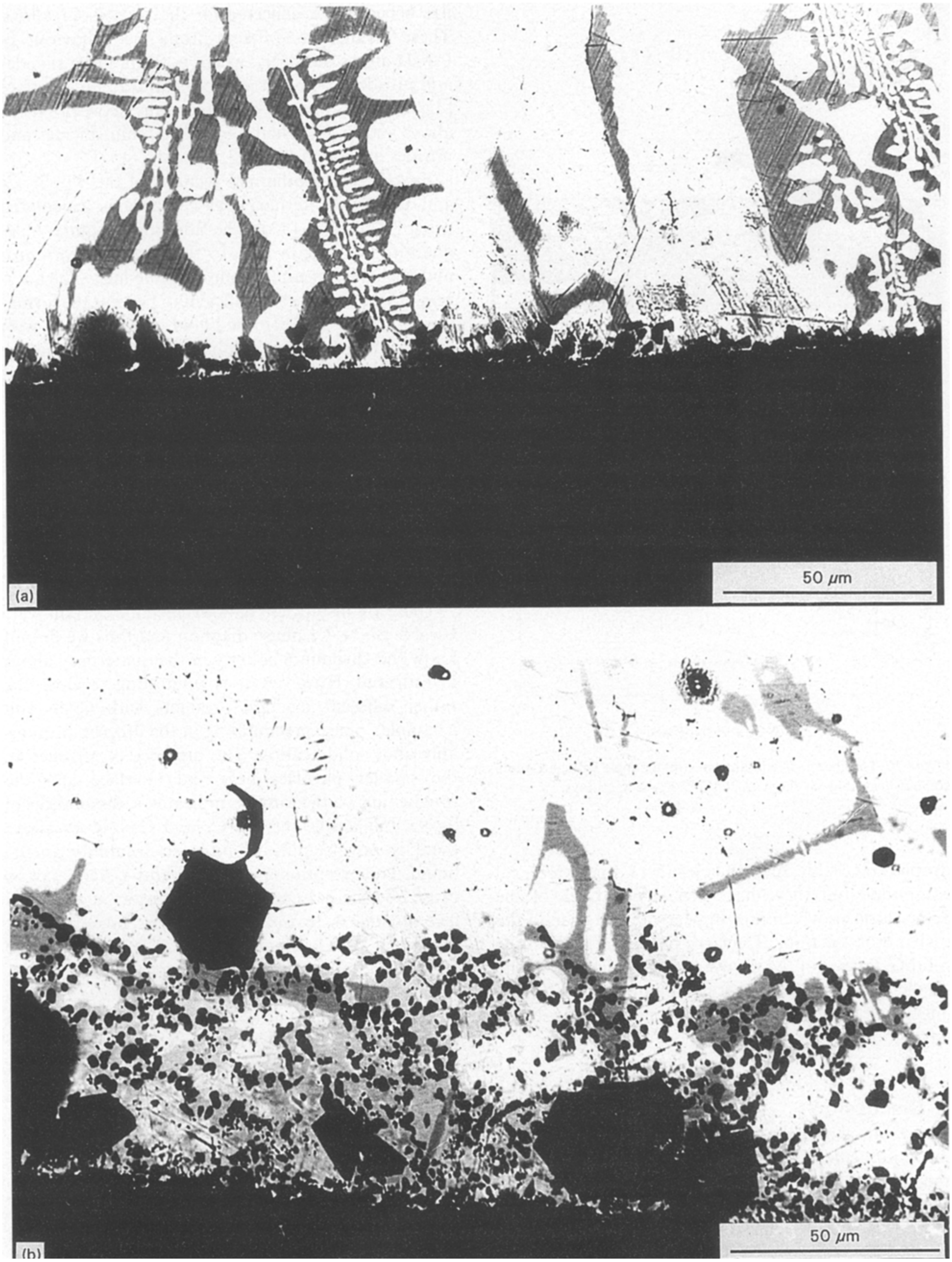

Figure 11 Interfacial cross-sections from (a) (Cu–20% Ni–5% Si–1.3% Cr)/Si_3N_4, (b) (Cu–20% Ni–5% Si–5%Cr)/Si_3N_4.

difficult to test this model on these systems. But it is reasonable to apply this model to a nitrides or carbides system because this model considers that the bonding at the interface (oxide/metal) is related to the bonding in the liquid solution of M–Me and of O–Me without considering the bonding character of the oxide substrate.

For the wetting of Si_3N_4 by liquid Cu–Cr alloys, the equilibrium contact angle observed is, in fact, the wetting of Cr_2N by liquid copper containing low con-

TABLE I The optimized model parameters of the liquid Cr–Cu alloys (J mol^{-1})

i/A_{ij}	A_{i0}	A_{i1}
0	62 797.75	− 18.951 86
1	1 183.91	0

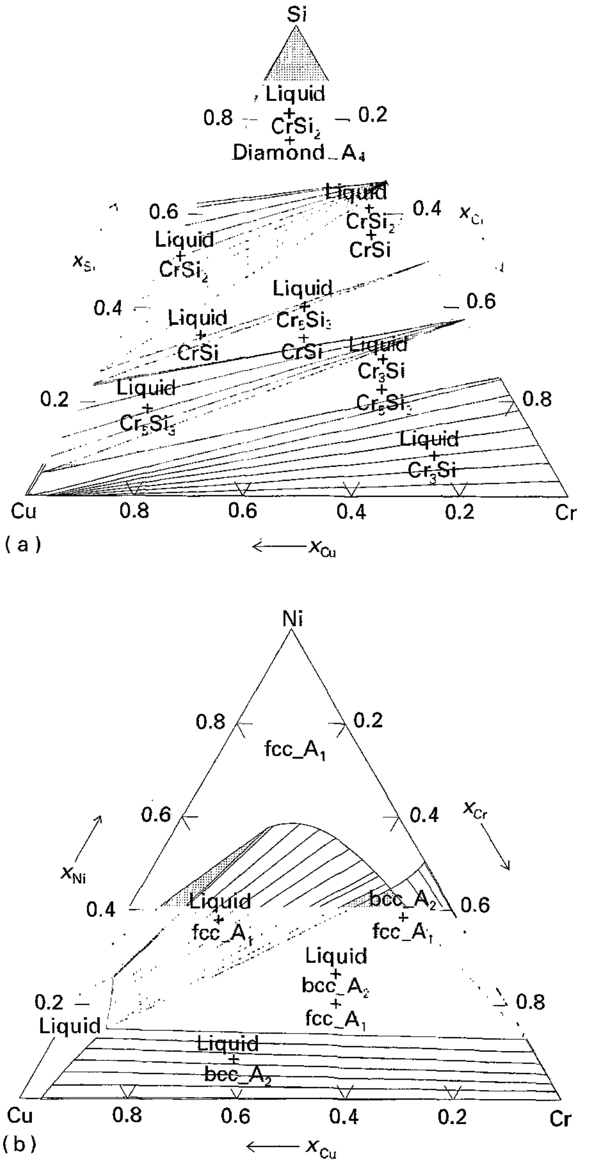

Figure 12 Isothermal sections of (a) the Cu–Si–Cr (b) Cu–Ni–Cr ternary phase diagrams at (a) 1433 and (b) 1473 K, respectively.

centrations of chromium. As a first approximation we can consider the wetting of the new interfacial phase by pure copper and use Equation 3 but with the species N rather than O. The Gibbs energy of nitrogen in liquid copper at 1 at % O is given as [10]

$$\Delta G_{\mathrm{N(M)}} = 69.2 - 0.018\,T\,(\mathrm{kJ\,mol^{-1}\,N})$$

$$= \Delta H^{0}_{\mathrm{N(Me)}} - T\Delta S^{0}_{\mathrm{N(Me)}} \qquad (4)$$

It is reasonable to assume that the enthalpy of mixing is independent of temperature, therefore, $\Delta H^{0}_{\mathrm{N(Cu)}}$ is 59 kJ. The value at infinite dilution, $\Delta H^{\infty}_{\mathrm{N(Cu)}}$, should be positive and close to $\Delta H^{0}_{\mathrm{N(Cu)}}$. A thermodynamic analysis of the Cu–Cr system gives the analytical form of the integral excess Gibbs energy as [14]

$$\Delta G_{\mathrm{ex}} = x_1 x_2 \Sigma A_j P_j(z) \qquad (5a)$$

$$A_i = A_{i0} + A_{i1}\cdot T \qquad (5b)$$

where x_1 and x_2 are the fractions of copper and chromium, A_{ij} are adjustable parameters which are given in Table I, $P_j(z)$ are the Legendre polynomials of degree j with argument z

$$z = x_1 - x_2 \qquad (6a)$$

$$P_0(z) = 1 \qquad (6b)$$

$$P_1(z) = x_1 - x_2 \qquad (6c)$$

$$p_2(z) = [3(x_1 - x_2)^2 - 1]/2 \qquad (6d)$$

From Equation 5a and b $\Delta H^{\infty}_{\mathrm{Cr(Cu)}}$ is calculated as 450 J. Thus both enthalpy terms in Equation 3 are positive and the work of adhesion is thus predicted negative. The work of adhesion is related to the contact angle by $W_{\mathrm{adh}} = \gamma_{\mathrm{LV}}(1 + \cos\theta)$. Thus the experimental results contradict the prediction of the model.

The failure of Chatain's model might be caused by a number of reasons. First, we are ignoring the effect of chromium and this may segregate to the interface and reduce its energy. Secondly, this model is developed for ionocovalent oxides and it has already been found to give a poor prediction of wetting on metallic oxides, e.g. TiO and Ti_2O_3 [15]. The metallic nature of refractory metal nitrides may partly explain the difference between model and experiment. However, the best wetting behaviour observed occurred with the Cu–Ni–Si–Cr alloy where no Cr_2N formed and the liquid was, presumably, in equilibrium with Si_3N_4.

5. Conclusion

The effect of chromium additions on the wetting of Si_3N_4 was determined using Cu–Cr, Cu–Ni–Cr, Cu–Si–Cr and Cu–Ni–Si–Cr alloys. The addition of chromium to all these alloys improved their wettability of Si_3N_4. However, wettability was also controlled by the maximum (saturation) chromium content in the liquid alloys. The addition of nickel to Cu–Cr increased the solubility of chromium and improved the wetting on Si_3N_4. Cr_2N formed at the interfaces of Cu–Cr/Si_3N_4 and of Cu–Ni–Cr/Si_3N_4. The addition of silicon to Cu–Cr suppressed the formation of Cr_2N at the metal/ceramic interface, but limited the chromium solubility because of the formation of the solid chromium silicides. Therefore, Cu–Si–Cr alloys did not have very good wetting on Si_3N_4. Cu–Ni–Si–Cr alloys were found to have very good wetting on Si_3N_4 without forming a continuous Cr_2N layer at the metal/ceramic interface. The presence of dissolved nitrogen may explain the improved wetting behaviour. More work is necessary to investigate the wetting of this complex alloy on Si_3N_4.

Simple models of wetting developed for oxides [16] do not correctly predict the behaviour observed in this study. Further work is necessary to extend these models to nitride systems.

References

1. M. G. NICHOLAS, D. A. MORTIMER, L. M. JONES and R. M. CRISPIN, *J. Mater. Sci.* **25** (1990) 2679.
2. D. H. KIM, S. H. HWANG and S. S. CHUN, *Ceramic. Int.* **16** (1990) 333.
3. P. KRISTALIS, L. COURDRIER and N. EUSTATHOPOULOS, *J. Mater. Sci.* **26** (1991) 3400.
4. M. G. NICHOLAS, in "Joining of Ceramics", edited by M. G. Nicholas, (Chapman and Hall, London, 1990) 73.
5. YU. NAIDICH, Prog. Surf. Memb. Sci. **14** (1981) 353.
6. P. XIAO and B. DERBY, *Acta Metall. Mater.* (1995) accepted.
7. P. KRISTALIS, V. MERLIN, L. COURDRIER and N. EUSTATHOPOULOS, *ibid.* **40** (1992) 1167.
8. D. J. CHAKRABARTI and D. E. LAUGHLIN *Bull. Alloy Phase Diagr.* **5** (1984) 59.
9. E. A. BRANDES and G. B. BROOK, "Smithells Metals Reference Book", 7th Edn (Butterworths, London, 1992).
10. Y. AUSTIN CHANG, K. FITZNER and MIN-XIAN ZHANG, *Prog. Mater. Sci.* **32** (1988) 97.
11. S. D. PETEVES, M. MOULAERT, and M. G. NICHOLAS, *Metall. Trans.* **23A** (1992) 1773.
12. M. NAKAMURA and S. D. PETEVES, *J. Am Ceram. Soc.* **73** (1990) 1221.
13. R. H. DAVIES, A. T. DINSDALE, T. G. CHART, T. I. BARRY and H. M. RAND, *High Temp. Sci.* **26** (1990) 251.
14. M. HAMALAINEN, K. JAJSKELAINEN, R. LUOMA, M. NUOTIO, P. TASKINEN and O. TEPPO, *CALPHAD* **14** (1990) 125.
15. P. KRITSALIS, B. DREVET, N. VALIGNAT and N. EUSTATHOPOULOS, *Script Metall. Mater.* **30** (1994) 1127.
16. D. CHATAIN, I. RIVOLLET and N. EUSTATHOPOULOS, J. Chim Phys. **83** (1986) 561.

Received 1 May
and accepted 7 June 1995